JOURNAL OF NEUROPHYSIOLOGY
Vol. 66, No. 5, November 1991. *Printed in U.S.A.*

Representation of Sensory Information in the Cricket Cercal Sensory System. I. Response Properties of the Primary Interneurons

JOHN P. MILLER, GWEN A. JACOBS, AND FRÉDÉRIC E. THEUNISSEN
Department of Molecular and Cell Biology, Division of Neurobiology, University of California, Berkeley, California 94720

SUMMARY AND CONCLUSIONS

1. Six different types of primary wind-sensitive interneurons in the cricket cercal sensory system were tested for their sensitivity to the orientation and peak velocity of unidirectional airflow stimuli.

2. The cells could be grouped into two distinct classes on the basis of their thresholds and static sensitivities to airflow velocity.

3. Four interneurons (the right and left 10-2 cells and the right and left 10-3 cells) made up one of the two distinct velocity sensitivity classes. The mean firing frequencies of these interneurons were proportional to the logarithm of peak stimulus velocity over the range from 0.02 to 2.0 cm/s.

4. The other two interneurons studied (left and right 9-3) had a higher air-current velocity threshold, near the saturation level of the 10-2 and 10-3 interneurons. The slope of the velocity sensitivity curve for the 9-3 interneurons was slightly greater than that for the 10-2 and 10-3 interneurons, extending the sensitivity range of the system as a whole to at least 100 cm/s.

5. All of the interneurons had broad, symmetrical, single-lobed directional sensitivity tuning curves that could be accurately represented as truncated sine waves with 360° period.

6. The four low-threshold interneurons (i.e., left and right 10-2 and 10-3) had peak directional sensitivities that were evenly spaced around the horizontal plane, and their overlapping tuning curves covered all possible air-current stimulus orientations. The variance in the cells' responses to identical repeated stimuli varied between ~10% at the optimal stimulus orientations and ~30% at the zero-crossing orientations.

7. The two higher threshold interneurons (left and right 9-3) had broader directional sensitivity curves and wider spacing, resulting in reduced overlap with respect to the low-threshold class.

INTRODUCTION

A general principle that has emerged from studies of the structure and function of sensory systems is that stimulus parameters, such as the spatial location of a visual or auditory point source, are often "mapped" continuously within layered arrays of neurons (Knudsen et al. 1987; Konishi 1986). Higher order interneurons that read such neural maps generally have stimulus-response characteristics that can be represented as parametric tuning curves; i.e., there will be a set of specific "optimal" stimulus parameters that elicit a "maximal" response from each interneuron,[1] and the cell's response will decrease in a continuous manner as any stimulus parameter is varied from the optimum. The width of a cell's tuning curve may be defined as the range of stimulus parameters around the optimum that elicit a significant response from the interneuron. Different interneurons naturally have slightly different peak tuning points and generally have tuning curves that are broader than the interneighbor spacing. Thus a particular stimulus that results in a sharp peak of activity in the map may influence activity in several or many higher order interneurons, depending on the extent of the overlap of their tuning curves. The relevant information about the sensory stimulus may be encoded within the conjoint activity of all of these higher order interneurons.

With these general principles in mind, questions arise concerning the inherent limits of accuracy in such a mapped sensory system. How is the systematic accuracy limited by the shapes, widths, and relative spacing (or "density") of the characteristic tuning curves of the constituent interneurons? How is systematic accuracy limited by variability in cell responses?

These are very difficult questions to answer and must ultimately be addressed in behavioral terms. A somewhat surprising result that has emerged from psychophysical studies in several different organisms (including humans) is that the degree of stimulus resolution observed at the behavioral level is generally finer than the widths or spacing of the tuning curves of the sensory receptors or interneurons at higher levels in the associated neural maps (for examples, see Rose and Heiligenberg 1986; Westheimer 1981). These questions have been addressed recently in several theoretical studies, in which "hyperacuity" could be achieved by a mechanism equivalent to interpolation of sensory stimulus values from the activity of neural units having widely spaced, broadly overlapping tuning curves (Baldi and Heiligenberg 1988; Heiligenberg 1987; Zhang and Miller 1991).

Here we addressed these questions from a slightly different approach in a relatively simple mapped sensory system. Rather than assessing the accuracy from observations of behavior, we directly assessed the inherent constraints on accuracy imposed by the characteristics of the neurons from which the system is constructed.

For these studies a preparation was used wherein the full range of a sensory parameter was covered by only four primary sensory interneurons that had broad, overlapping tuning curves equally spaced throughout the parameter

[1] The "maximal response" is often difficult to define. In cells having substantial baseline activity levels, a significant amount of information about the stimulus might be encoded as a change in the firing pattern, rather than as simply a change in the mean firing rate as is usually assumed (for several examples see Eckhorn and Popel 1975; Fuller and Looft 1984; Optican and Richmond 1987; Richmond and Optican 1990; de Ruyter van Steveninck and Bialek 1988; Segundo et al. 1963.

space. The preparation we studied was the cercal sensory system of the common house cricket *Acheta domestica*. Crickets (and many other orthopteran insects) have two antenna-like appendages at the rear of their abdomen, each of which is covered with hundreds of filiform hair mechanoreceptors. Each hair is coupled at its base to a single sensory neuron (Gnatzy and Tautz 1980; Palka et al. 1977), and the sensory system mediates the detection and analysis of air-current stimuli in the animal's immediate environment (Bacon and Murphey 1984; Edwards and Palka 1974; Jacobs et al. 1986; Tobias and Murphey 1979). The structure of the cuticular hinge at the base of each hair constrains motion to a single plane (Gnatzy and Tautz 1980). When the hair is displaced in one direction in this plane, the rate of action-potential generation in the associated sensory cell increases. Hair displacement in the opposite direction causes a reduction below the base level firing rate. The thousand or so hairs on each cercus are arranged in many different orientations, insuring that several hairs will be displaced for any possible air-current stimulus direction. The afferent axons of all the filiform mechanosensory receptors project into the terminal abdominal ganglion and arborize within two bilaterally symmetric regions called the cercal glomeruli (Bacon and Murphey 1984). The projection of these afferents is topographic with respect to the positions of the mechanosensory hairs on the cercus (Bacon and Murphey 1984; Walthall and Murphey 1986); and, as a consequence, a map of air-current direction is formed within the glomeruli.

The cells that carry information about air-current direction out of the ganglion to higher centers are primary sensory interneurons that receive direct excitatory synapses from the afferents (Bacon and Murphey 1984; Shepherd and Murphey 1986). At least 10 different bilaterally symmetric pairs of these projecting interneurons have been identified (Mendenhall and Murphey 1974; Jacobs and Murphey 1987), and the directionally selective response properties of several of these cells have been studied (Bacon and Murphey 1984; Jacobs and Miller 1985; Jacobs et al. 1986). However, none of these studies were designed specifically to examine the system's accuracy in determining wind stimulus orientation. In the experiments reported here, appropriate measurements were made of the directional sensitivities and response variances of a subset of these primary sensory interneurons. Specifically, we have characterized the directional sensitivity tuning curves of two cell types in a class that has not previously been described in this species: left 10-2 and right 10-2 (according to the nomenclature defined in Jacobs and Murphey 1987). We have also remeasured the directional sensitivity of four other cell types with greater precision than had been possible in earlier studies: left and right 10-3 (Jacobs et al. 1986) and left and right 9-3 (Bacon and Murphey 1984). We found that the interneurons have symmetrical, unimodal, overlapping tuning curves. Moreover, we found that the tuning curves had relatively small response variances and small interanimal variabilities.

On the basis of these measurements and on conservative assumptions about information coding, principles of information theory were applied to calculate the limit of directional accuracy that can be achieved in this system. Those results are presented in the second paper in this series.

METHODS

Dissection and preparation of specimens

All experiments were performed on adult female crickets (*A. domestica*) obtained from a local supplier (Bassett's Cricket Ranch, Visalia, CA). Specimens were selected that had undergone their final molt within 4–24 h. The head, legs, wings, and ovipositor were removed from each specimen, and a thin flap of cuticle was removed from the dorsal surface of the abdomen. After removal of the gut, the body cavity was rinsed and subsequently perfused with hypotonic saline (O'Shea and Adams 1981). Hypotonicity facilitated microelectrode penetration of the ganglionic sheath.

The preparation was pinned to a thin slab of silicone elastomer (Sylgard; Dow Chemical) that had approximately the same projectional area as the cricket's abdomen. To reduce the turbulence at the specimen's cerci caused by obstruction of air movement beneath the preparation, special care was taken in pinning the animal to this slab in two respects. First, the abdomen was pinned such that the two cerci were completely extended over the rear of the slab, so that there was no material directly below any part of the cerci to disrupt local airflow laminarity. Second, the abdomen was suspended 2–4 mm *above* the Sylgard slab on the four minuten pins used to mount the preparation, at a height similar to the normal "standing" height observed when legs are intact. This insured that air could move under and around the abdomen, rather than being obstructed and forced to flow back across the cerci. Figure 1 shows a typical preparation mounted for electrophysiological recording.

The response properties of interneurons recorded in preparations mounted in this manner were significantly different from

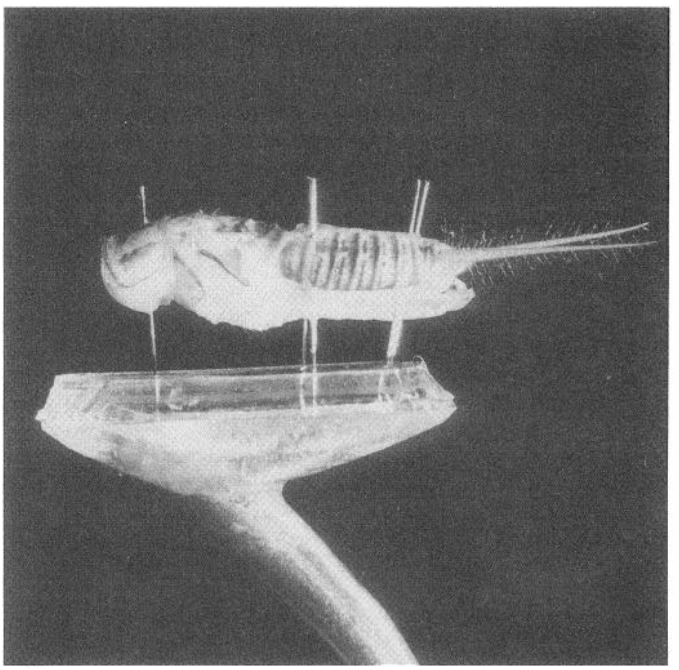

FIG. 1. Photograph of the semi-intact preparation mounted above a Sylgard slab on the recording platform. Note the minimal obstruction to airflow in the vicinity of the cerci, which are the 2 antenna-like appendages at the posterior end of the abdomen. Many of the mechanosensory filiform hairs can be seen on the cerci.

those recorded from preparations mounted directly onto platforms that restricted subabdomenal and subcercal airflow, in two main respects (data not shown). First, the response to several identical stimuli was less variable in the elevated preparations. Second, the directional sensitivity tuning curves (see Fig. 5) of the interneurons were narrower and more symmetrical in the elevated preparations. Both of these results indicate that there was significantly less turbulence and less air-current obstruction in the elevated preparations.

Wind stimulus generator

In previous studies of directional sensitivity using these interneurons, air-current stimuli were delivered from nozzles directed at the preparations from distances greater than the nozzle diameters (Bacon and Murphey 1984; Jacobs and Miller 1985; Jacobs et al. 1986). This results in turbulent, nonlaminar air flow at the cerci. To circumvent these problems, a wind tunnel was constructed within which laminar air-current stimuli with precisely controlled direction and velocity parameters could be generated. The wind tunnel was constructed from Plexiglas tubing with 2-in inside diameter. Each end of the wind tunnel was connected through a large-diameter Tygon tube to a different chamber. An 8-in diam loud speaker was mounted on each chamber, such that movement of the speakers would drive air through the tubes into the tunnel. The two speakers were driven reciprocally by identical voltage waveforms to generate a unified "push-pull" displacement of the air within the tunnel. At the extremely low driving frequencies (2 Hz) used for these experiments, there were no measurable disturbances of the airflow attributable to any resonnances, which might be expected to arise when two mechanically independent speakers are used.

The wind tunnel and speaker apparatus was a closed system, except for *1*) a small hole in the tunnel below the preparation for entry of the pedestal support for the small Sylgard mounting slab and *2*) a small hole in the tunnel directly above the cricket for insertion of glass capillary microelectrodes. The tunnel was mounted on a carousel and could be rotated 180° around the preparation in the horizontal plane without disturbing intracellular recordings. By generating 2 stimuli with opposite polarities at each of 8 positions around the 180° range of the device, 16 directional responses were routinely recorded at 22.5° increments to cover the entire 360° range.

The voltage waveforms used to drive the speakers were generated by a digital waveform synthesizer (RC Electronics, Santa Barbara, CA) mounted in a microcomputer (IBM PC/AT). Waveforms of arbitrary shape and amplitude could be constructed. Typical waveforms included voltage ramps (yielding step changes of constant velocity) and half cycles of cosine waves (yielding half-cycle sine waves). Peak air-current velocity was varied by changing the amplitude of the driving waveform. The relationship between the voltage waveform used to drive the speakers and the resulting air-current velocity was determined in a set of calibration experiments (i.e., without a preparation mounted) by measuring the air-current velocity with a microbridge mass airflow sensor (Microswitch No. AWM 2300). This device was extremely sensitive and linear within the frequency and velocity ranges used in these experiments: the "roll-off" frequency for the sensor was 200 Hz, and stimulus velocities were measurable to within 5% accuracy over the whole range used in our studies. (We note that hot wire anemometers are neither accurate nor linear for airflow velocities <10 cm/s and could not be used with confidence.) In the studies reported here, half-sine stimulus waveforms of 2 Hz were used for all measurements unless otherwise noted. With the use of the airflow sensor described above, the time course of the speaker-generated air-current stimuli was determined to reproduce these sinusoidal voltage waveforms with no measurable distortion or phase lag.

It is important to note that this wind-tunnel apparatus was capable of generating sustained, unidirectional air displacements, rather than being limited to bidirectional, oscillating displacements (i.e., "tones") as in previous studies (Edwards and Palka 1974; Levine and Murphey 1980; Shimozawa and Kanou 1984). Unidirectional stimuli were achieved by *1*) "cocking" the speakers in one direction, *2*) holding them there until neuronal activity returned to baseline levels, *3*) generating the desired stimulus by driving the speakers to their other extreme with the appropriate voltage waveform, *4*) holding the speakers at that extreme for an adequate time for neuronal activity to recover, and *5*) returning the speakers to their initial rest position.

Intracellular recording

The small Sylgard slab, above which the cricket was pinned, was placed within the wind tunnel on a thin platform having the same projectional area as the Sylgard slab. The terminal ganglion was stabilized on a miniature spoon introduced through the hole in the top of the wind tunnel and held rigid by a micromanipulator. The ganglionic sheath was partially digested with a 3% solution of protease (Sigma) in standard hypotonic saline.

Microelectrodes were filled with either 3% Lucifer yellow (Sigma) in 2 M lithium chloride or 3% carboxyfluorescein (Kodak) in 2 M potassium acetate and had resistances ranging from 10 to 30 MΩ. Electrical activity was recorded with a Dagan 8800 electrometer in bridge mode. Data were acquired and analyzed with an RC Electronics ISC-16 data acquisition system synchronized with the wind stimulus waveform generator.

For cell identification, dye was iontophoresed into the neuron with 3 nA of hyperpolarizing current for 10 min and visualized in situ with an epifluorescence attachment to a Wild M5 stereo microscope.

RESULTS

The terminal abdominal ganglion contains at least 10 different pairs of primary sensory interneurons that receive direct excitatory input from filiform afferents (Bacon and Murphey 1984; Edwards and Palka 1974). Each of these pairs consists of two mirror-symmetric, bilaterally homologous cells. In the experiments reported here, intracellular recordings were obtained from the left and right homologues of three of these different cell classes: interneurons 10-2, 10-3, and 9-3 (Jacobs and Murphey 1987; Mendenhall and Murphey 1974).

Most recordings were from cell bodies, although several recordings were obtained from neuropil processes within the cercal glomerulus. In no case was an overshooting action potential observed. Spikes were always attenuated to between 3 and 20 mV, suggesting that the somatic and dendritic membranes are passive. Overshooting spikes could, however, be recorded from axons of these cells in the interganglionic connectives, by the use of electrodes prepared in an identical manner to those used for cell body recordings. This suggests that the inability to record overshooting spikes from cell bodies was not an artifact of electrode damage.

Resting potentials of all cells ranged from −55 to −65 mV. Cell types 10-2 and 10-3 showed average spontaneous firing rates of ~2 Hz. The 9-3 cells showed no significant spontaneous activity.

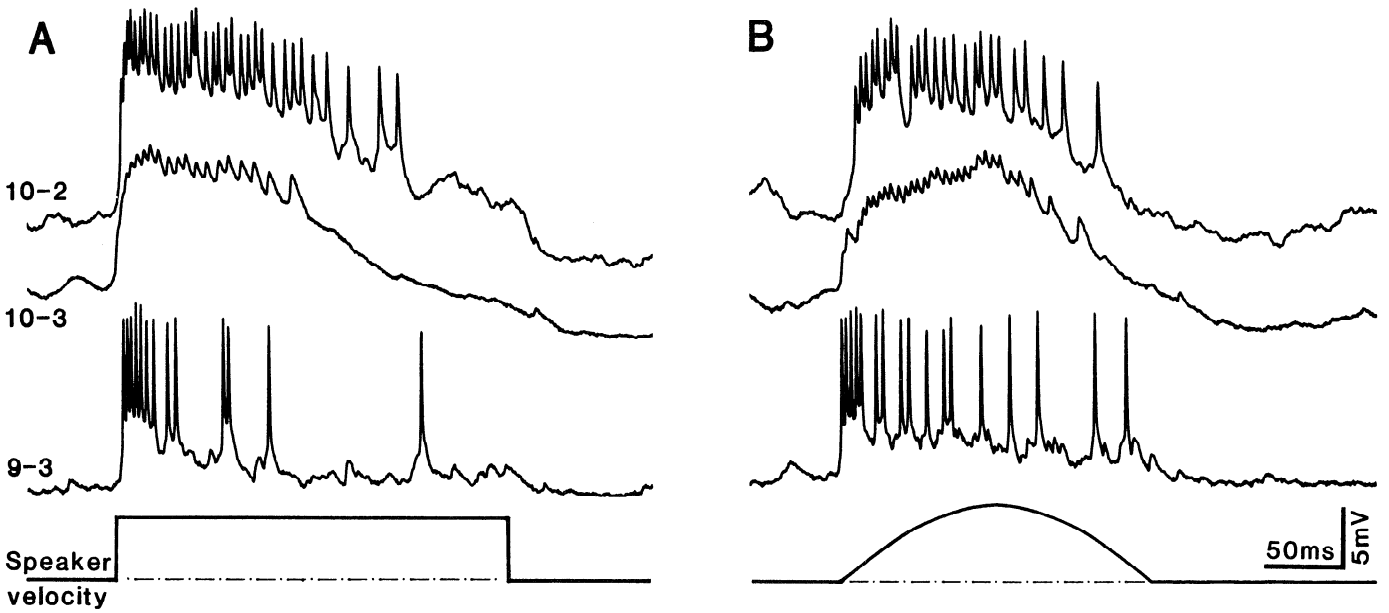

FIG. 2. Typical responses of the different interneuron types to air-current stimuli. The cell responses were elicited by air currents oriented to the optimal direction for each cell type. The recordings from the 10-3 cell were obtained from the cell body, and the recordings from the 10-2 and 9-3 cells were obtained from neuropil penetrations. Peak air-current velocities were as follows: cells 10-2 and 10-3, 0.15 cm/s; cell 9-3, 0.6 cm/s. *A*: responses to air currents generated by constant velocity speaker displacements. *B*: responses to stimuli with velocity proportional to ½ cycle of a sine wave.

Typical responses to wind stimuli, oriented to the optimal direction for each cell, are shown in Fig. 2. The wind stimuli used in *A* were step increases from zero to a constant velocity. The velocity versus time of the wind stimuli in *B* was proportional to one-half cycle of a sine wave. These half-sine waveforms were used for all subsequent experiments.

Velocity sensitivity

Our main goal in these studies was to characterize the directional sensitivity of these cells. However, to ensure that we were using stimuli of appropriate amplitude (i.e., significantly above threshold but below saturation), responses were first recorded for a series of wind stimuli that had the same direction and duration but that had logarithmically increasing peak velocities. For all measurements the wind tunnel was oriented to the optimal direction for the particular cell under study. Note that these half-period sinusoidal stimuli were unidirectional, i.e., the air currents advanced in one direction with no "return stroke." Control experiments carried out with stimuli shaped to yield constant velocity and constant acceleration air currents yielded similar static sensitivity curves (data not shown). For the first-order analysis presented in this study, the response amplitudes of each cell were simply calculated as the number of action potentials generated during each stimulus. These values were then scaled to the maximum number of spikes generated by that particular cell.

The solid-line curve in Fig. 3*A* shows a plot of the scaled response amplitude versus peak stimulus velocity for a typical 10-3 cell. Each data point is the mean of two measurements, taken at 15-s intervals to avoid accomodation. Note the error bars on the point taken at a wind velocity of 1.7

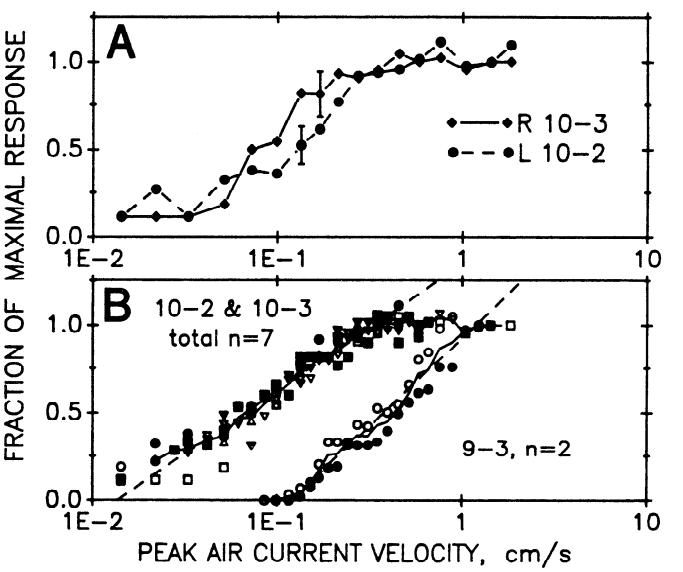

FIG. 3. Velocity sensitivity of the interneurons. *A*: the solid curve is a plot of the scaled response amplitude of a right 10-3 cell vs. peak air-current velocity. The mean peak response at saturation for this cell (i.e., scaled as 1.0) was 21 spikes per 250-ms stimulus. The error bar at the stimulus velocity of 0.17 cm/s was the standard deviation of 20 trials; all other points are the average of 2 trials. The dashed curve is a plot of the sensitivity of a left 10-2 cell under an identical protocol. In this case, the mean peak response at saturation was 20 spikes per 250-ms stimulus. The error bar at a velocity of 1.4 mm/s represents the standard deviation of 20 repeated measurements at this velocity. *B*: mean sensitivities of the different cell classes to air-current stimuli of different peak velocities. The solid curve in the *left data set* is the lumped mean of the responses from 7 different "10" cells: 2 left 10-3 cells, 2 right 10-3 cells, 2 left 10-2 cells, and 1 right 10-2 cell. The dashed line through this data set is the least-squares fit to the points between stimulus velocities of 0.03 and 0.23 cm/s. The solid curve in the *right data set* is the mean of the response of 2 "9" cells: a left 9-3 and a right 9-3. The dashed line is a least-squares fit to the data points between 0.17 and 0.7 cm/s.

mm/s. At this velocity, 20 measurements were taken to assess the variability of the cell's response to repeated stimuli. The error bars represent ±1 standard deviation from the mean value. It was impractical to record this many measurements at each wind velocity, but the relatively small standard deviation suggests that a mean of two samples yielded a reasonable estimate.

The dashed curve in Fig. 3*A* shows the responses of a 10-2 cell to the same stimulus set. The error bar at a velocity of 1.4 mm/s represents the standard deviation of 20 repeated measurements at this velocity. The curves for interneurons 10-2 and 10-3 lie well within one standard deviation of one another over the whole range of measurement and were thereby judged to be insignificantly different. From similar data recorded from other cells, it was determined that there were no significant differences in the velocity sensitivity curves for left and right homologues of the same cell types (i.e., left and right 10-2 were indistinguishable, left and right 10-3 were indistinguishable, and left and right 9-3 were indistinguishable).

Figure 3*B* shows the scaled responses of seven different 10-2 and 10-3 cells (*left curve*) and two 9-3 cells (*right curve*). The line through each data point set is a least-squares fit to the points between the 10 and 90% response levels. Note that the 9-3 cells have a higher threshold than the 10-2 and 10-3 cells. The slopes of the velocity sensitivity response curves of the 9-3 cells are slightly greater than those of the 10-2 and 10-3 cells.

Directional sensitivities

The directional sensitivity of each of the six cell types was measured by recording its response to airflow stimuli from

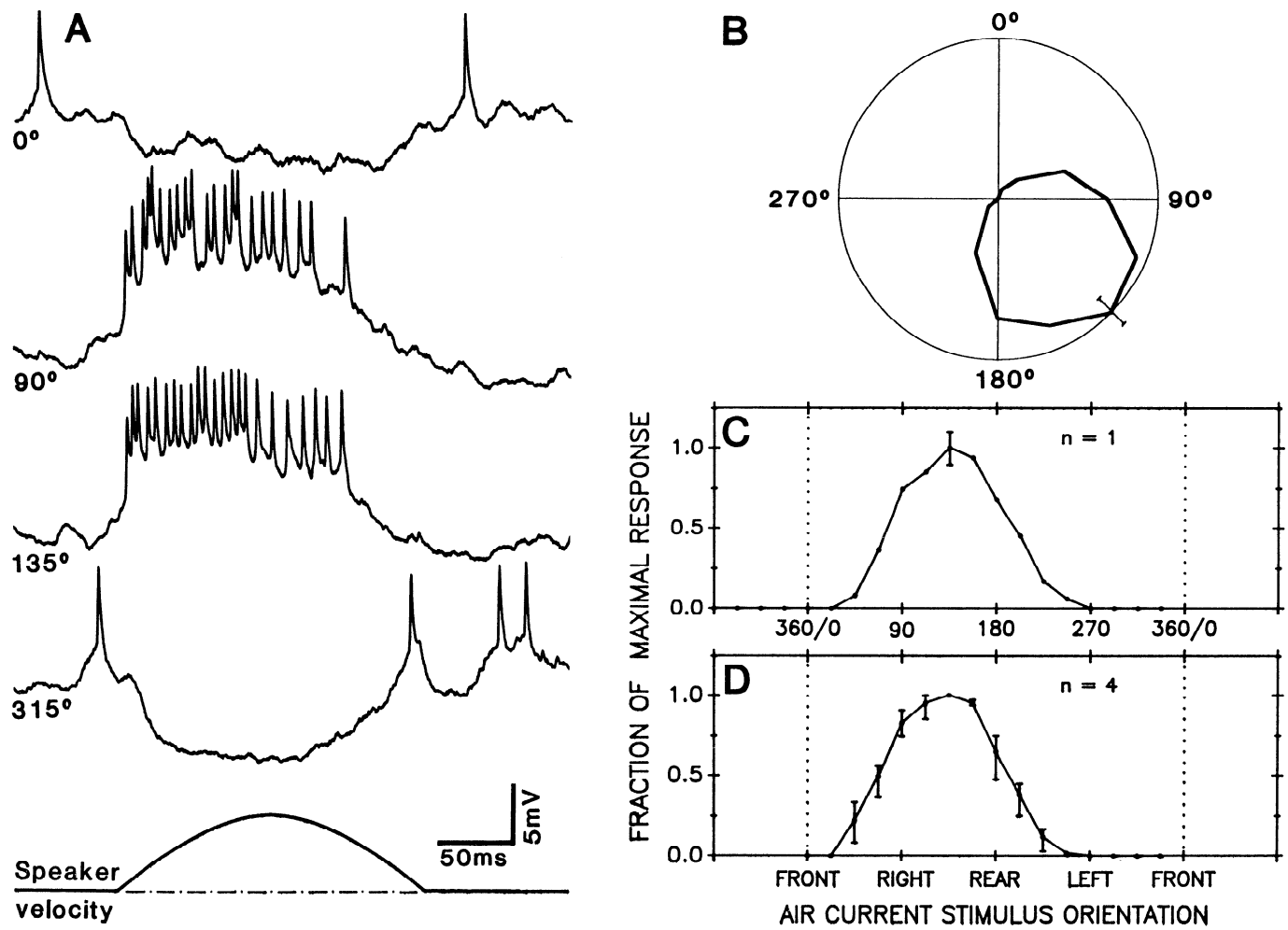

FIG. 4. Directional sensitivity of a right 10-2 cell. *A*: responses of the cell to 4 different air-current stimuli having identical velocity profiles but different orientations. Stimulus orientations are indicated as degrees clockwise from directly in front of the animal. *B*: polar plot of the mean spike rate of right 10-2 vs. stimulus orientation. All responses were scaled to the maximal response rate of 20 spikes per stimulus interval, elicited at a stimulus orientation of 135°. The outer circle represents the scaled maximum response value of 1.0, and the origin represents a rate of 0. Because responses were quantified in terms of spike rate and resting rates were near zero, the inhibitory responses were not represented in these plots. The error bar at the optimal orientation is the standard deviation of 20 measurements. All other points represent the mean of 4 measurements. *C*: this is the same data as plotted in *B*, but plotted in Cartesian coordinates. Note that the graph wraps around: the stimulus orientation corresponding to the front of the animal is represented twice on the graph. *D*: mean directional sensitivity curve calculated from 4 different left 10-2 cells. Each individual curve was scaled to its own maximal response before averaging with the other curves. Error bars indicate the total range of mean responses at each stimulus orientation, and *not* the variance of individual cell responses.

16 different orientations in the horizontal plane. For these experiments, the only parameter of the stimulus that was changed was the orientation; the velocity profile of the airflow was identical for all orientations and was proportional to one-half cycle of a sine wave. The peak velocity of the airflow stimuli in each experiment was adjusted to elicit a response that was between 50 and 75% of the cell's maximum (i.e., saturation) response level at its optimal stimulus orientation, as determined from the data plotted in Fig. 3*B*.

All of the cell types displayed definite directional tuning. Examples of typical responses recorded from a 10-2 cell during wind stimuli from four different orientations are shown in Fig. 4*A*. Note that stimuli from some orientations evoke a depolarization and burst of action potentials in the cell, whereas stimuli from other directions result in a hyperpolarization of the cell membrane potential to a value below the resting level.

The directional sensitivity of the cell from which these data were recorded is plotted in Fig. 4, *B* and *C*. For these plots, the response amplitudes of the cell at each direction was quantified by averaging the number of action potentials generated during four identical wind stimuli and scaling that mean response to the maximum response obtained at the optimal stimulus orientation. In this case the mean optimal response was 20 spikes, obtained when the air current was directed at 135° clockwise from the front of the animal. This response value was scaled as 1.0.

The data are plotted in two different formats. In Fig. 4*B*, the data are graphed in polar coordinates, according to the conventions used in previous studies on this system (Bacon and Murphey 1984; Edwards and Palka 1974; Jacobs et al. 1986; Levine and Murphey 1980). In *C*, the data are plotted in cartesian coordinates, rather than in polar coordinates. Note that the data are "wrapped around," such that the region at the front of the animal is represented twice on the graph. This format for plotting the data has distinct advantages over polar plots by allowing a much clearer visualization of the optimal direction, relative "breadth," and symmetry of the tuning curves. Note that the tuning curve is single lobed, symmetric, and oriented to the right rear quadrant of the animal's environment. The tuning curve is relatively broad, with a width at half-maximal response of 123°.

In general, electrode recordings could not be maintained for long enough periods to obtain more than four trials at each stimulus orientation. However, additional responses were measured at one stimulus orientation to assess the variance to repeated identical stimuli. The error bar at the optimal response orientation in Fig. 4*C* represents the standard deviation calculated from 20 responses (SD, 11% of the mean response).

Directional sensitivity curves were measured in this manner from four left 10-2 cells. The curves were all very similar in shape, with mean peak responses that varied from 18 to 20 spikes per stimulus. To obtain a representation of the mean directional sensitivity for all of these left 10-2 cells, the four individual curves were scaled to their maximal responses and averaged to obtain the curve shown in Fig. 4*D*. Note that the error bars on this curve represent the total range of mean responses at each stimulus orientation, and not the variance of the cell responses themselves. (i.e., the absence of error bars at the optimal response orientation indicates that all four cells had their mean peak responses at this same stimulus orientation. Note, as mentioned above, that the variance of a typical left 10-2 cell to repeated stimuli at this direction was 11% of the mean.)

Directional tuning curves were measured from the six different cell types (left and right 10-2, left and right 10-3, left and right 9-3). For each of these cell types, a mean directional sensitivity plot was obtained by averaging the scaled tuning curves from between three and six different preparations. These mean directional tuning curves are plotted in Fig. 5. In Fig. 5, just as in Fig. 4*D*, the error bars represent the range in the mean responses at each stimulus orientation, and not the variance of individual cell responses. The relatively small error bars indicate a small interanimal variability.

These plots have been segregated into two different classes, corresponding to the two classes defined earlier in terms of the velocity sensitivities. For the four-member class of 10-2 and 10-3 cells, the spacing between peak sensitivity points was 90°, and the mean width at half-maximal response was 124°. For the two-member class of 9-3 cells, the separation was 148°, and the width at half-maximal response was 138°. In all cells, the directional tuning curves were single lobed and symmetric around the optimal stimulus orientation.

Variability in the responses of the interneurons

A determination of the accuracy attainable by any sensory system requires a knowledge of the variability in each cell's responses to identical repeated stimuli. Experiments were therefore performed to calculate the variance at as many different stimulus orientations as possible in each of several 10-2 and 10-3 cells. At each stimulus orientation, 32

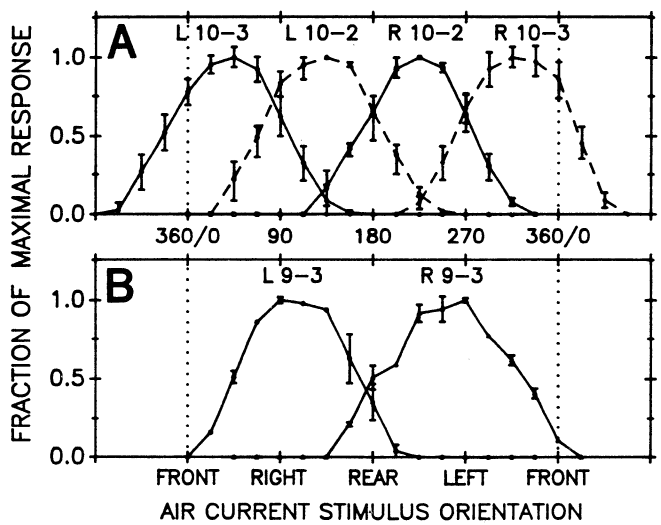

FIG. 5. Directional sensitivity tuning curves for all 6 cell types. For each cell type, a mean directional sensitivity plot was obtained by averaging the scaled tuning curves from between 3 and 6 different preparations, as was done for Fig. 4*D*. Error bars represent the range in mean responses at each stimulus orientation, and *not* the variance of individual cell responses. *A*: directional curves for the 10-2 and 10-3 cells. *B*: directional curves for the 9-3 cells.

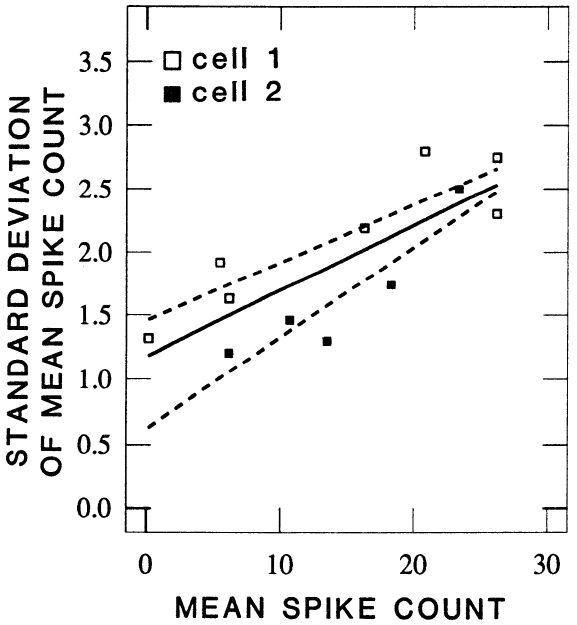

FIG. 6. Variance in individual cell responses to identical repeated stimuli. The x-axis is the mean response amplitude, quantified as the number of spikes elicited per stimulus. The y-axis is the *variance* in the response, quantified as the standard deviation of the spike count in a set of responses. Each point represents the calculated variance in a cell's response to 32 repeated stimuli at a particular direction. Response variances vs. mean responses are plotted for 2 different cells: a left 10-3 (*cell 1*) and a right 10-2 (*cell 2*). These 2 curves represent the limiting cases (i.e., minimal and maximal observed variances). The lines through the data sets represent the best linear fits. R^2 values were 0.80 and 0.82 for the *top* and *bottom plots*, respectively.

stimulus-response trials were recorded. The number of different stimulus orientations that could be tested in each cell was limited by the duration of intracellular electrode penetrations. The results of two such experiments are shown in Fig. 6, where the standard deviation of the spike count is plotted against the mean spike count for several different directions in each of two cells. These two cases represented the limiting cases (i.e., minimal and maximal observed variances). In each cell, the data could be fit reasonably well with a linear function, in which the standard deviation increased proportionally to the mean response amplitude. The variance at the optimal response orientations (i.e., a variance of ~2.5 spikes for a mean response of ~25 spikes) corresponded to a relative variance of ~10%.

Analytic functions equivalent to the directional tuning curves

The four directional tuning curves of the 10-2 and 10-3 cells, shown in Fig. 5*A*, were used to create a "grand mean" tuning curve. This was done by shifting the individual curves to align their means and taking the average of the four different values at each 22.5° interval away from this mean. Figure 7*A* shows the mean values of these four curves (□) and the associated standard deviations. The standard deviations of the mean responses are much smaller than the variances of the individual cell responses at the corresponding stimulus orientation as shown in Fig. 6. The directional tuning curves from different cells were therefore judged to be statistically indistinguishable.

The solid line in Fig. 7*A* is the best fit to these data points of the following functions

$$r = [r_{max}/(1 - a_t)]*[\cos(\theta - \theta_{max}) - a_t] \quad \text{for} \quad \cos(\theta - \theta_{max}) > a_t \quad (1a)$$

and

$$r = 0 \quad \text{for} \quad \cos(\theta - \theta_{max}) < a_t \quad (1b)$$

where r is the response amplitude (i.e., mean spike count),

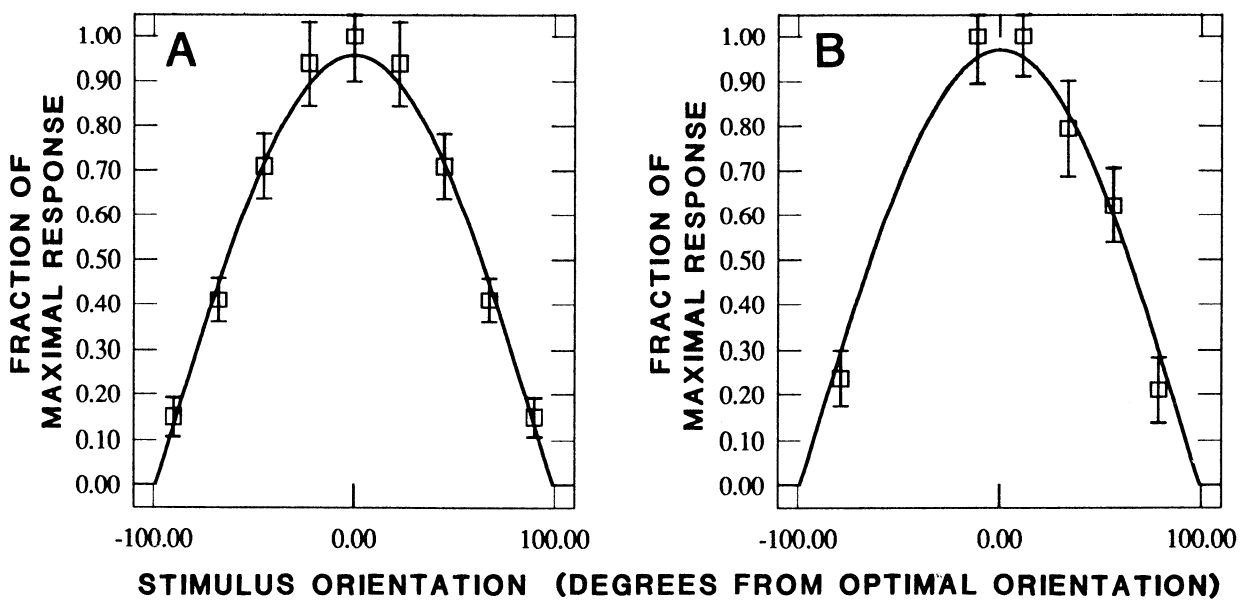

FIG. 7. Model function fitted to the mean directional tuning curves. *A*: each data point is the average of mean responses from all 10-2 and 10-3 tuning curves shown in Fig. 5*A*, shifted appropriately to align their means. Error bars are the standard deviation of the mean responses. The curve through the data points was obtained with a value of −0.14 for alpha in *Eq. 1a* of the text. *B*: each data point is the mean of 32 responses at a particular stimulus orientation for a left 10-3 cell. Error bars are the response variance. Responses were recorded for 6 different directions in this cell. The curve through the points is the same function that was fit to the grand mean directional curve plotted in *A*.

r_{max} is the maximum response amplitude; θ is the stimulus direction in radians; θ_{max} is the optimal stimulus direction evoking the maximum response; and a_t is the threshold stimulus value for evoking spike activity.

This is a simple cosine function with spatial period of 360°, truncated at some "threshold" level a_t, and scaled to have a "peak-to-truncation" magnitude of r_{max}. The response function r can be thought of as being the resultant sum of excitation from sensory receptor afferents and inhibition from local interneurons. The threshold value is presumably determined by the relative amount of excitation and inhibition, as well as by the spike threshold of the interneurons. The $[r_{max}/(1-a_t)]$ coefficient can be thought of as a gain factor. With r_{max} normalized to a value of 1, the only free parameter that was actually adjusted to fit this function to the measured data points was a_t, which was set to a value of -0.14 for these data points.

Note that this curve fell within one standard deviation of the mean responses at all stimulus orientations. The normalized χ^2 value for the fit is less than one, indicating that the analytic expression is an adequate representation of the mean data. The width of this model tuning curve at half-maximum amplitude was 130°.

Figure 7*B* shows this same curve superimposed on the data set for directional sensitivity of a single left 10-3 cell. The recording from this cell was maintained long enough to obtain 32 repetitions at each of 6 different directions, allowing a calculation of the response variance (indicated with error bars) at these sample directions. Here again, the analytic curve derived from the data plotted in *A* fell within one standard deviation of the mean responses, and the normalized χ^2 value was less than one for the fit. This demonstrates that the fit is valid for a typical individual tuning curve, as well as for the group mean.

DISCUSSION

The electrophysiological results reported in this paper demonstrate aspects of the directional sensitivity of six types of primary sensory interneurons in the cercal system of the cricket *A. domestica* to low-velocity, unidirectional air-current stimuli. The neurons could be divided into two groups, based on their thresholds and sensitivities to the air-current stimuli. Neurons in both groups had broad, symmetrical, overlapping directional sensitivity tuning curves that could be accurately represented as truncated sine waves.

When the four curves of the 10-2 and 10-3 interneurons were superimposed by alignment of their medians, their differences in shape were statistically insignificant. The mean of these four curves was fit very well by a truncated sine wave with a period of 360°. The sinusoidal form and 360° period of these interneurons' tuning curves is exactly as should be expected from a consideration of the Fourier theorem. Because of the mechanics of the cuticular hinge at the base of each hair (Gnatzy and Tautz 1980; Landolfa et al. 1988), the directional tuning curves of the mechanosensory receptors are also nearly perfectly sinusoidal with spatial periods of 360°. These mechanoreceptor tuning curves should be considered the "basis function set" from which the tuning curves of the first-order sensory interneurons are synthesized, and the Fourier theorem states that any function synthesized through a linear summation of such basis functions could itself only be a sinusoidal function with the same period.

The only nonlinear aspect of the summation, i.e., the truncation, is due presumably to two factors. The first factor that would be expected to contribute to response truncation is simply the characteristics of the interneurons' spike initiation kinetics: each interneuron needs some finite level of activation by afferent inputs before any action potentials can be elicited. The second factor is the involvement of polysynaptic inhibitory inputs onto the interneurons, activated by air-current stimuli from some directions (Jacobs et al. 1986; Levine and Murphey 1980), which act to shunt the membrane potentials to below threshold for spike activation.

Although the sinusoidal form and period of the interneuron tuning curves were as anticipated, the precise uniformity of shape of the 10-2 and 10-3 cell tuning curves and the uniform "placement" of their peak sensitivity points at 90° intervals around the stimulus range is noteworthy in several respects. As demonstrated in earlier reports (Bacon and Murphey 1984; Jacobs and Miller 1985; Jacobs et al. 1986), the shape and placement of a cell's directional tuning curve depends on three factors. First, the excitatory receptive field of a cell is constrained by the location of its dendrites within the complex topographic afferent map of wind direction that exists within the cercal glomeruli. Second, the relative synaptic efficacy of afferent inputs from hairs of different directional sensitivity onto the interneuron's different dendritic branches is determined by the length and diameter (or "electroanatomy") of the dendritic segments connecting those branches to the spike initiation zone. Third, as mentioned above, inhibitory inputs from local interneurons are thought to play a significant role in shaping the directional sensitivity curves of some of these cells (Jacobs et al. 1986; Levine and Murphey 1980). If we consider the structural complexity of the afferent map (Jacobs and Poy 1990; Walthall and Murphey 1986) and the complexity of the dendritic structure of these cells (Jacobs and Murphey 1987), the similarity in the degree of truncation and the extremely uniform placement of these tuning curves around the stimulus range seems quite remarkable. Presumably, even a slight alteration in *1*) the locations of an interneuron's dendrites within the afferent map, *2*) the transfer impedances between those dendritic input sites and the spike initiation zone, or *3*) any aspects of the inhibitory input onto the cell would alter the apparent width (i.e., degree of "truncation" of the sine wave) and/or the position of peak sensitivity. Modeling studies are currently underway to determine more quantitatively the degree to which the shape and placement of a cell's tuning curve depends on slight alterations in these parameters.

Comparison with previous studies

The velocity thresholds and sensitivities of interneurons homologous to the ones studied here have been examined

in a different species of cricket: *Gryllus bimaculatus* (Kanou and Shimozawa 1984). In that study the experimental chamber and measurement conditions were very similar to those used in the studies reported here, except for the use of a hot wire anemometer (in earlier studies) versus a solid-state mass airflow sensor (in the current studies) for calibration of the wind stimulus velocities. The wind velocity threshold reported for the 10-2 and 10-3 cells in those earlier studies was ~50 μm/s at 2 Hz, compared with our measurements of ~200 μm/s in *A. domestica*. Thresholds of the 9-3 cells in the earlier studies were measured to be between 10 and 30 mm/s, compared with 2 mm/s in our current studies. These measurements should be considered to be in excellent agreement, considering *1*) the crickets studied were from two different genera, *2*) the ambient background noise levels were not explicitly measured nor controlled in either study and may have contributed to different levels of adaptation, and *3*) the reliability of hot wire anemometers and mass airflow sensors in making absolute determinations of air velocity is relatively poor at such low flow rates.

Velocity sensitivity of these or any homologous cells have not been carried out in any other studies by protocols that are sufficiently similar to justify comparison. In any case it is impossible to know a priori what the relevant parameters of the cells' responses are in terms of their encoding of information about stimulus velocity; therefore our characterizations were done solely to determine an appropriate suprathreshold, subsaturation stimulus velocity range adequate for our measurements.

Measurements of the directional sensitivity based on mean spike rates elicited by unidirectional stimuli have been reported previously for right 9-3 (Bacon and Murphey 1984) and for right 10-3 (Jacobs et al. 1986). Although the earlier results are in general agreement with the current report, experimental measurement conditions were not equivalent. In the case of right 9-3, the measurements were taken in a situation where all sensory hairs on the left cercus were immobilized with petroleum jelly (Vaseline). Moreover, in both earlier studies, the air-current stimuli were generated with air jets projected from nozzles in open field conditions. There are two problems with such configurations that make the results unsuitable for the analysis of response variance. First, the air currents generated by a nozzle become turbulent within a distance equivalent to the nozzle orifice diameter. Second, because the preparations were not enclosed within air tunnels in those earlier studies, the ambient air currents may also have been significantly above threshold for activation of these cells. Both sources of noise would be expected to have artifactually increased the observed variance in the cells' responses and to have broadened the apparent tuning curves.

We note that two factors in our own studies reported here may have altered some significant factors affecting the baseline of accuracy that would presumably be observed in a freely behaving cricket. First, we used a relatively "noise-free" stimulus generator. A cricket's normal air-current environment would be expected to display some background noise and "drift," and some behaviorally relevant stimuli might be expected to display some degree of turbulence. Although the use of noise-free stimuli is perfectly valid from an engineering analysis standpoint, it should be remembered that the cercal system's performance in the field might be significantly affected by such factors. We are currently assessing the influence of stimulus noise and drift on system accuracy. Second, several structures were removed from each preparation (i.e., the head, wings, legs, and ovipositor), which might normally be expected to influence air currents around the animal's body. The removal of the legs and ovipositor would presumably increase the streamlining of airflow near the cerci, whereas removal of the head and wing covers would be expected to decrease the streamlining of airflow around our preparations with respect to the normal case. Considering the very low air-current velocities used in these studies, we suspect that these effects are, however, not significant.

Structure and operation of the system

The projecting interneurons in the cercal sensory system, including the 10-2, 10-3, and 9-3 cells studied here, can be easily stained and identified by backfilling the abdominal connectives with cobalt or other suitable dyes. With the use of these techniques, other right/left pairs of primary sensory interneurons have been identified that have dendrites within the filiform cercal glomeruli and have axons that project up the connectives to higher CNS centers. If we consider the sensitivity of these histological techniques, it is unlikely that many more (if any) projecting interneurons remain to be identified that could carry additional information about wind stimuli to higher centers. During the course of these experiments, electrode penetrations were obtained from all types of projecting interneurons that have been identified to date. None except the 10-2 and 10-3 cells were observed to display obvious directional sensitivity within the range of stimulus amplitudes equivalent to that spanned by 10-2 and 10-3, according to the criteria used in this study (i.e., a dependence of the mean spike rate following a stimulus on the direction of the stimulus). We note, however, that information about stimulus orientation could be encoded in characteristics of neuronal spike trains other than their mean firing rate following a stimulus, as has been found to be the case in several other studies (for several examples see Eckhorn and Popel 1975; Fuller and Looft 1984; Optican and Richmond 1987; Richmond and Optican 1990; de Ruyter van Steveninck and Bialek 1988; Segundo et al. 1963). For example, an interneuron might exist that would generate equal numbers of spikes in response to stimuli from all orientations, but that could encode information about direction in the onset latency, peak frequency, or some other higher order statistical characteristics of the spike train. Our criteria for directional selectivity would have missed such a cell; these possibilities will be dealt with in a subsequent report.

In any case, the number of interneurons carrying information about wind stimuli to higher centers is still very restricted. At least one additional type of cells (probably "9-2"), having a threshold and velocity sensitivity equivalent to that of the 9-3 cells, was observed to display directional sensitivity, but an adequate number of recordings for

a statistically significant characterization were not obtained. And it is known from other studies that at least two types of cells (the "medial giants" and "lateral giants") display directional sensitivity within a range of velocities even greater than that spanned by the 9-3 cells (Bacon and Murphey 1984).

Thus it appears that the interneurons that are definitely capable of conveying information about wind direction can be subdivided into at least three groups of as few as four cells each, and that each group could conceivably encode information about the direction of wind stimuli within a different range of peak stimulus velocities. The overlap of these velocity sensitivity ranges could guarantee the maintenance of directional sensitivity over a wide dynamic range of velocities (and/or accelerations).

This system may therefore represent an excellent preparation for the study of "coarse coding." The whole stimulus range of 360° of possible stimulus directions within any particular velocity range may be fractionated between only four sensory interneurons, all of which have relatively broad, overlapping tuning curves. It will be interesting to determine whether the cricket is capable of hyperacuity, i.e., the ability to localize the direction of wind stimuli with a degree of accuracy exceeding the interreceptor spacing of 90°.

Although behavioral studies will be essential to an analysis of the accuracy of this system, the following companion paper offers an alternate approach to the questions associated with the accuracy of this system and with the specific mechanisms underlying its operation. Rather than formulating these questions in terms of any specific (and necessarily ad hoc) models for system operation and neural coding scheme, principles of information theory were used to calculate a conservative estimate of the upper limit of accuracy that the system could possibly attain.

This work was supported by National Science Foundation Grant BNS-8519416 to J. P. Miller.

Address for reprint requests: J. P. Miller, Dept. of Molecular and Cell Biology, Life Sciences Addition, Box 193, University of California, Berkeley, CA 94720.

Received 28 November 1990; accepted in final form 12 June 1991.

REFERENCES

BACON, J. P. AND MURPHEY, R. K. Receptive fields of cricket (*Acheta domesticus*) interneurones are determined by their dendritic structure. *J. Physiol. Lond.* 352: 601–618, 1984.

BALDI, P. AND HEILIGENBERG, W. How sensory maps could enhance resolution through ordered arrangements of broadly tuned receivers. *Biol. Cybern.* 59: 313–318, 1988.

ECKHORN, R. AND PÖPEL, B. Rigorous and extended application of information theory to the afferent visual system of the cat. II. Experimental results. *Biol. Cybern.* 17: 7–17, 1975.

EDWARDS, J. S. AND PALKA, J. The cerci and abdominal giant fibers of the house cricket, *Acheta domesticus*. I. Anatomy and physiology of normal adults. *Proc. R. Soc. Lond. B Biol. Sci.* 185: 83–103, 1974.

FULLER, M. S. AND LOOFT, F. J. An information theoretic analysis of cutaneous receptor responses. *IEEE Trans. Biomed. Eng.* 31.4: 377–383, 1984.

GNATZY, W. AND TAUTZ, J. Ultrastructure and mechanical properties of an insect mechanoreceptor: stimulus-transmitting structures and sensory apparatus of the cercal filliform hairs of *Gryllus*. *Cell Tissue Res.* 213: 441–463, 1980.

HEILIGENBERG, W. Central processing of sensory information in electric fish. *J. Comp. Physiol. A* 161: 621–631, 1987.

JACOBS, G. A. AND MILLER, J. P. Functional properties of individual neuronal branches isolated in situ by laser photoinactivation. *Science Wash. DC* 228: 344–346, 1985.

JACOBS, G. A., MILLER, J. P., AND MURPHEY, R. K. Cellular mechanisms underlying directional sensitivity of an identified sensory interneuron. *J. Neurosci.* 6: 2298–2311, 1986.

JACOBS, G. A. AND MURPHEY, R. K. Segmental origins of the cricket giant interneuron system. *J. Comp. Neurol.* 265: 145–147, 1987.

JACOBS, G. A. AND POY, N. S. J. Quantitative analysis of topographic mapping in the cricket cercal sensory system. *Soc. Neurosci. Abstr.* 16: 401, 1990.

KANOU, M. AND SHIMOZAWA, T. A threshold analysis of cricket cercal interneurons by an alternating air-current stimulus. *J. Comp. Physiol. A* 154: 357–365, 1984.

KNUDSEN, E. I., DULAC, S., AND ESTERLY, S. D. Computational maps in the brain. *Annu. Rev. Neurosci.* 10: 41–65, 1987.

KONISHI, M. Centrally synthesized maps of sensory space. *Trends Neurosci.* 9: 163–168, 1986.

LANDOLFA, M. A., JACOBS, G. A., AND MILLER, J. P. Input-output relationships of sensory afferent neurons in the cricket cercal sensory system. *Soc. Neurosci. Abstr.* 14: 379, 1988.

LEVINE, R. B. AND MURPHEY, R. K. Pre- and postsynaptic inhibition of identified giant interneurons in the cricket (*Acheta domesticus*). *J. Comp. Physiol.* 135: 269–282, 1980.

MENDENHALL, B. AND MURPHEY, R. K. The morphology of cricket giant interneurons. *J. Neurobiol.* 5: 565–580, 1974.

OPTICAN, L. M. AND RICHMOND, B. J. Temporal encoding of two-dimensional patterns by single units in primate inferior temporal cortex. III. Information theoretic analysis. *J. Neurophysiol.* 57: 163–178, 1987.

O'SHEA, M. AND ADAMS, M. E. Pentapetide (proctolin) associated with an identified neuron. *Science Wash. DC* 213: 567–569, 1981.

PALKA, J., LEVINE, R., AND SCHUBIGER, M. The cercus-to-giant interneuron system of crickets. I. Some aspects of the sensory cells. *J. Comp. Physiol.* 119: 267–283, 1977.

RICHMOND, B. J. AND OPTICAN, L. M. Temporal encoding of two-dimensional patterns by single units in the primate primary visual cortex. II. Information transmission. *J. Neurophysiol.* 64: 370–380, 1990.

ROSE, G. J. AND HEILIGENBERG, W. Limits of phase and amplitude sensitivity in the torus semicircularis of *Eigenmania*. *J. Comp. Physiol. A* 159: 813–822, 1986.

DE RUYTER VAN STEVENINCK, R. R., AND BIALEK, W. Real time performance of a movement sensitive neuron in the blowfly visual system: coding and information transfer in short sequences. *Proc. R. Soc. Lond. B Biol. Sci.* 234: 379–403, 1988.

SEGUNDO, J. P., MOORE, G. P., STENSAAS, L. J., AND BULLOCK, T. H. Sensitivity of neurones in *Aplysia* to temporal pattern of arriving impulses. *J. Exp. Biol.* 40: 643–667, 1963.

SHEPHERD, D. AND MURPHEY, R. K. Competition regulates the efficacy of an identified synapse in crickets. *J. Neurosci.* 6: 3152–3160, 1986.

SHIMOZAWA, T. AND KANOU, M. Varieties of filiform hairs: range fractionation by sensory afferents and cercal interneurons of a cricket. *J. Comp. Physiol. A* 155: 485–493, 1984.

TOBIAS, M. AND MURPHEY, R. K. The response of cercal receptors and identified interneurons in the cricket (*Acheta domesticus*) to air streams. *J. Comp. Physiol.* 129: 51–59, 1979.

WALTHALL, W. W. AND MURPHEY, R. K. Positional information, compartments and the cercal system of crickets. *Dev. Biol.* 113: 182–200, 1986.

WESTHEIMER, G. Visual hyperacuity. *Prog. Sens. Physiol.* 1: 1–30, 1981.

ZHANG, J. AND MILLER, J. P. A mathematical model for resolution enhancement in layered sensory systems. *Biol. Cybern.* 64: 357–364, 1991.